http://dx.doi.org/10.5012/bkcs.2012.33.3.911

Potential of Mean Force Calculations for Ion Selectivity in a Cyclic Peptide Nanotube†

Kyu-Min Choi, Chan Ho Kwon, Hong Lae Kim, and Hyonseok Hwang*

*Department of Chemistry and Institute for Molecular Science and Fusion Technology, Kangwon National University, Chuncheon, Gangwon-do 200-701, Korea. *E-mail: hhwang@kangwon.ac.kr*
Received December 7, 2011, Accepted January 5, 2012

Ion selectivity in a simple cyclic peptide nanotube, composed of four cyclo[-(D-Ala-Glu-D-Ala-Gln)$_2$-] units, is investigated by calculating the PMF profiles of Na^+, K^+, and Cl^- ions permeating through the peptide nanotube in water. The final PMF profiles of the ions obtained from the umbrella sampling (US) method show an excellent agreement with those from the thermodynamic integration (TI) method. The PMF profiles of Na^+ and K^+ display free energy wells while the PMF curve of Cl^- features free energy barriers, indicating the selectivity of the cyclic peptide nanotube to cations. Decomposition of the total mean force into the contribution from each component in the system is also accomplished by using the TI method. The mean force decomposition profiles of Na^+ and K^+ demonstrate that the dehydration free energy barriers by water molecules near the channel entrance and inside the channel are completely compensated for by attractive electrostatic interactions between the cations and carbonyl oxygens in the nanotube. In the case of Cl^-, the dehydration free energy barriers are not eliminated by an interaction between the anion and the peptide nanotube, leading to the high free energy barriers in the PMF profile. Calculations of the coordination numbers of the ions with oxygen atoms pertaining to either water molecules or carbonyl groups in the peptide nanotube reveal that the stabilization of the cations in the midplane regions of the nanotube arises from the favorable interaction of the cations with the negatively charged carbonyl oxygens.

Key Words : Cyclic peptide nanotube, Ion selectivity, Molecular dynamics simulation, Potential of mean force, Umbrella sampling

Introduction

Ion channels, which is a class of transmembrane proteins, have drawn great attention because they play a significant role in nerve and muscle excitation, sensory transduction, and hormone secretion.[1,2] One issue related to the functions of ion channels is the selectivity of ion channels to specific ions.[3] For instance, KcsA ion channels allow much more K^+ ions to translocate through themselves than other ions, and Na ion channels are more permeable to Na^+ and less permeable to K^+. Although the structure of ion channels is a crucial factor in elucidating ion selectivity in ion channels, energetics of ion transport through ion channels is considered to be another factor to modulate the selectivity.

Investigation of the free energy variation with respect to ion species inside ion channels can provide insight into ion selectivity in ion channels. In this sense, potential of mean force (PMF) calculations is an excellent means for understanding the selectivity as well as the energetics in ion permeation through ion channels. There have been a great number of computational studies to obtain the PMF profiles for ion transport through natural ion channels.[4-7] A problem arising from the PMF calculations of ions inside natural ion channels is that occasionally they are too complicated to interpret.

Cyclic peptide nanotubes are a synthetic ion channel that self-assemble through intermolecular hydrogen bonds between closed peptide rings composed of alternating D- and L-amino acids.[8-12] Depending on the hydrophilic or hydrophobic nature of the side chain of amino acids, the cyclic peptide nanotubes can be found either in water solution or in lipid bilayers. Due to their properties related to ion transport, they have been considered to be an antibacterial agent or a potential ion sensor.[13,14]

From a theoretical and computational point of view, cyclic peptide nanotubes are a reliable target system to examine the ion selectivity of ion channels because cyclic peptide nanotubes bear structural and functional resemblance to natural ion channels despite their simple structure. Several theoretical and computational studies have been done to better understand the dynamics and energetics of ion transport through the cyclic peptide nanotubes.[15-20] Asthagiri and Bashford calculated the excess free energy of several ions inside a simple cyclic peptide nanotube.[16] Hwang *et al.* used steered molecular dynamics (SMD) simulations to obtain the PMF profiles of a single Na^+ or K^+ ion in a cyclic peptide nanotube with hydrophilic side chains in water.[19] PMF profiles for a Na^+ through a cyclic peptide nanotube in water and in a lipid bilayer haven been determined using the adaptive biasing force (ABF) method by Dehez *et al*.[20]

In this work, we examine the ion selectivity in a simple cyclic peptide nanotube with respect to the energetics of the transport of three different ion species: Na^+, K^+, and Cl^-. To

†This paper is to commemorate Professor Kook Joe Shin's honourable retirement.

do so, the potential of mean force (PMF) profiles of the ions are constructed by performing molecular dynamics (MD) simulations and by using the umbrella sampling (US) and thermodynamic integration (TI) methods. The ion selectivity of the cyclic peptide nanotube to specific ions is discussed on the basis of the PMF profiles of the ions.

The paper is organized as follows. In the next section the target system is introduced and a couple of computational methods to obtain and construct PMF profiles are briefly reviewed. Results and discussion are presented in section III and concluding remarks are made in the final section. Limitations of the present work and further studies are also discussed in that section.

Computational Methods

Description of the Simulations. We consider a system consisting of a cyclic peptide nanotube, a single ion, and water molecules. The cyclic peptide nanotube used in the current study is formed by four cyclo[-(D-Ala-Glu-D-Ala-Gln)$_2$-] units (Figure 1).[8] In Figure 1, the alpha-plane regions are defined as the regions near the plane of the alpha-carbons in the peptide nanotube and the midplane regions are as the regions between two alpha-plane regions. Owing to the hydrophilic side chains, the peptide nanotube can dissolve in water. The protonated form of the glutamic acids initiates self-assembly of the cyclic peptide nanotube in water, and as a result, all the side chains of the glutamic acids in the peptide tube were protonated. The initial structure of the nanotube was adopted from Ref. 19. One difference in the structure compared with the one in the reference is that in the current study the side chains of the glutamic acids (glutamines) are facing the side chains of the glutamines (glutamic acids) in the next ring, while in the reference the side chains of one amino residue are facing the side chains of the same residue in the next ring. The CHARMM27 force field and TIP3P water model were employed to describe the cyclic peptide and water molecules.[21,22] The force field for the ions was obtained from Beglov and Roux.[23] Energy minimization of the peptide nanotube was performed to obtain an optimized structure of the tube. In the energy-minimized structure, the average distance between two adjacent rings is 4.71 Å and the average radius of a ring from the channel axis to alpha-carbons is 4.90 Å. The channel axis of the energy-minimized structure was oriented parallel to the z direction and the orientation of this structure was used as a reference to restrain the orientation of the nanotube in the MD simulations. After energy minimization, the Na^+, K^+, or Cl^- ion was introduced at a position along the z-axis of the nanotube, and water molecules were randomly positioned and oriented. The number of water molecules in the system was calculated on the basis of a partial volume of 1.00 cm^3/g for water and 0.73 cm^3/g for the nanotube.[15] The water molecules that have poor van der Waals interactions with the peptide nanotube or the ion were removed. Another energy minimization of the final system was conducted to avoid any unfavorable interactions between the molecules. The final system contains one nanotube, one ion, and 1130 water molecules in a simulation box whose size is 31.5 Å × 31.5 Å × 38.0 Å in x, y, and z directions, respectively.

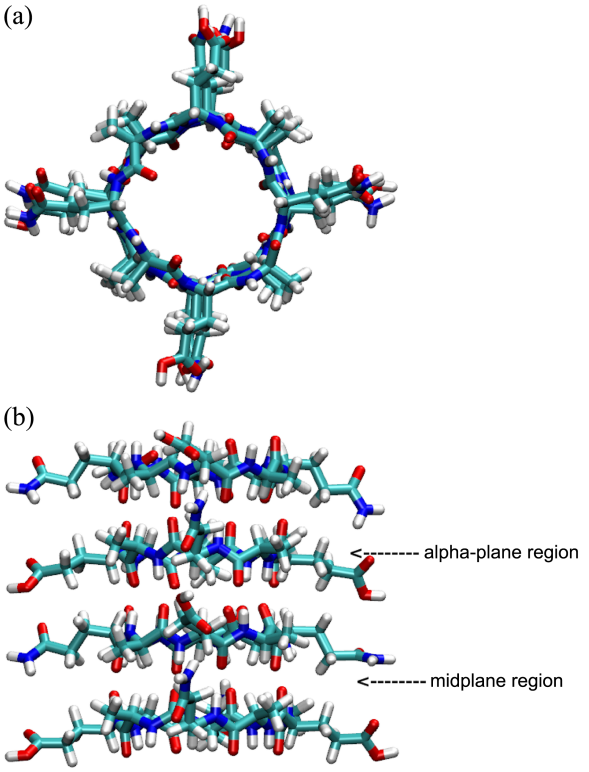

Figure 1. (a) Top view and (b) side view of a cyclic peptide nanotube, 4 × cyclo[-(D-Ala-Glu-D-Ala-Gln)$_2$-]. The alpha-plane regions and midplane regions are defined in the text following the work in Ref. 15.

All the MD simulations were carried out using the canonical (NVT) ensemble with periodic boundary conditions. A Langevin dynamics method with a damping constant of 5 ps^{-1} was used to maintain the temperature of the system at 298 K. The equations of motion was integrated with a time step of 2 fs for the equilibrations and PMF calculations. The SHAKE algorithm was employed to restrain the bonds between hydrogen atoms and their parent atoms. Long-range electrostatic interactions were treated using the particle mesh Ewald (PME) method with conducting boundary conditions. A cutoff distance of 12 Å was used for the evaluation of the real space sum of the Coulomb interaction. The reciprocal space sum in the Coulomb interaction was calculated on a grid of 32 × 32 × 40 points. Van der Waals interactions were truncated at 12 Å and were smoothly switched to 0 from 10 to 12 Å. The orientation of the channel axis of the nanotube was restrained in the z direction. For the calculation of the PMF profiles of the ions as a function of the ion position along the z direction, the center of mass of the alpha carbons in each ring unit was restrained in the z direction with a harmonic spring constant of 25 kcal/mol/Å^2, but the tube was allowed to move freely in x and y directions. All the energy minimizations and MD simulations were performed using the NAMD 2.8,[24] and visualizations were made possible using the VMD 1.8.6.[25]

PMF Constructions. Several methods have been proposed and developed for the calculation of PMF profiles.[26,27] In the current study we use two methods to obtain and compare the PMF profiles for the ion transport through the cyclic peptide nanotube. One of the methods that we used is the umbrella sampling (US) method via the weighted histogram analysis method (WHAM).[28] Since detailed explanations of the US method is elsewhere,[27,28] a brief review is just presented here. In the US method, the reaction coordinate is divided by a number of windows and the biased distribution of the reaction coordinate in each window is calculated from a series of MD simulations with a harmonic window potential. Then, the biased distributions are combined and unbiased using the WHAM procedure to construct the final unbiased PMF as:

$$\Delta A(z) = A_i(z) - A_0(z) = -k_BT \ln\left(\frac{\tilde{P}_i(z)}{\tilde{P}_0(z)}\right) - k_BT \ln\left(\frac{\langle e^{-w_i(z)/k_BT}\rangle}{\langle e^{-w_0(z)/k_BT}\rangle}\right) - w_i(z) + w_0(z), \quad (1)$$

where $A_0(z)$ is the Helmholtz free energy at the reference position, and $\tilde{P}_i(z)$ and $w_i(z)$ are the biased distribution function and umbrella window with the form $w_i(z) = k(z - z_i)^2$ at the ith window.

The other method we employed in this work is the thermodynamic integration (TI) method where the PMF, which is just a reversible work done by the ion, is calculated directly by integrating the mean force acting on the ion in the z direction:

$$\Delta A(z) = A_i(z) - A_0(z) = -\int_{z_0}^{z_i} \langle F(z)\rangle_z dz, \quad (2)$$

where $F(z)$ is the force acting on the ion at position z.[29]

To construct the PMF profiles from the US method, we take as the reaction coordinate the channel axis parallel to the z direction. The reaction coordinate is divided by 151 windows with a width of 0.2 Å from −15.1 Å to 15.1 Å and a harmonic window potential with a force constant of 25 kcal/mol/Å^2 is applied to restrain the ions in the window. For convergence, 1 ns of trajectory generation was performed for each window, where the ions are first equilibrated for 0.5 ns and the ion positions are sampled every 4 fs during 0.5 ns production runs. For the PMF constructions, the biased distributions of the ion positions are postprocessed using the WHAM implementation by Grossfield.[30] For the PMF calculation based on the TI technique, the coordinates of all the atoms in the system are collected every 400 fs during the 0.5 ns production runs of the biased MD simulations for the US sampling. The forces acting on the ions are calculated from the collected configurations and averaged as a function of the ion position.

One advantage of the TI method over the US method is that the TI method enables us to decompose the total PMF into the contribution from each component consisting of the system as:

$$\Delta A_\alpha(z) = A_{\alpha,i}(z) - A_{\alpha,0}(z) = -\int_{z_0}^{z_i} \langle F_\alpha(z)\rangle_z dz, \quad (3)$$

where $F_\alpha(z)$ is the force acting on the ion by a component α. The decomposition of the mean force is made possible by computing and integrating the mean force on the ion by the cyclic peptide nanotube and water separately. The MD trajectories and thereby all the PMF curves and PMF decomposition profiles were calculated four times independently. The final symmetrized PMF profiles shown in the next section were reconstructed by creating duplicate windows on opposite sides of the channel and by averaging the eight individual unsymmetrical PMF curves.

Results and Discussion

Figure 2 depicts the four individual unsymmetrical PMF curves and the final symmetrized PMF profiles of a single Na^+ ion through the cyclic peptide nanotube obtained from the US and TI methods independently. It is interesting that although the final PMF profiles are alike, the individual PMF curves obtained from the one method are different from the curves from the other method. The PMF profiles in Figure 2 demonstrate that the PMF construction from a single MD trajectory does not guarantee the accuracy in the resulting PMF profile. Based on the comparison between the results from the two method, it is required to average at least four independent PMF profiles to acquire reasonable final PMF profiles in our calculations where the coordinate of the ion was sampled every 4 fs during 0.5 ns production runs in

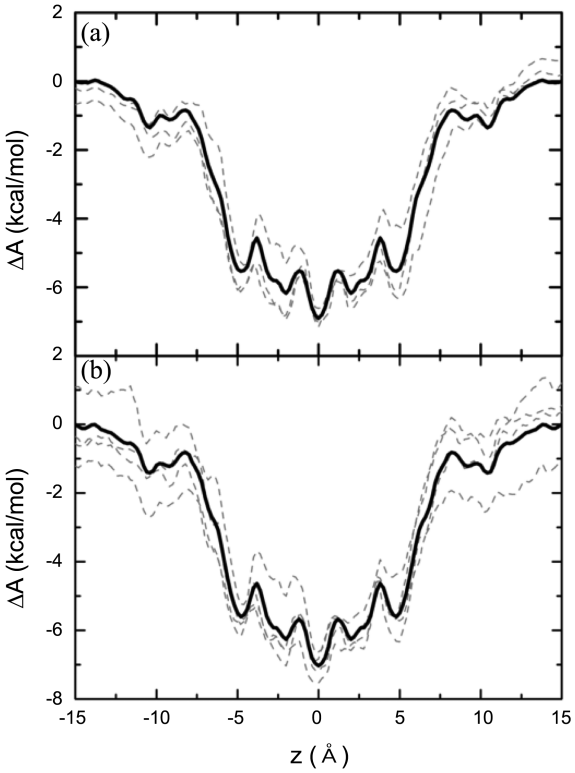

Figure 2. Final symmetrized PMF profiles of a single Na^+ ion obtained from the (a) US and (b) TI methods independently. The broken lines represent four individual PMF profiles. The final PMF profiles were obtained by averaging and symmetrizing the four individual unsymmetrical PMF curves.

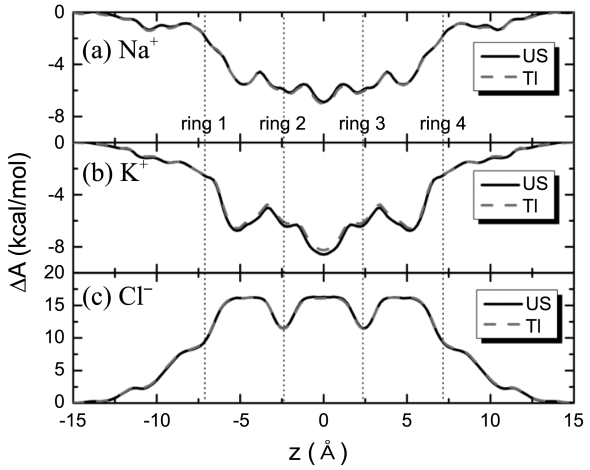

Figure 3. PMF profiles of (a) Na^+, (b) K^+, and (c) Cl^- as a function of the ion position in the *z* direction parallel to the channel axis. The PMF profiles were obtained independently by both the US and the TI methods. The dot lines indicate the position of the center of mass of the eight α carbons in each ring.

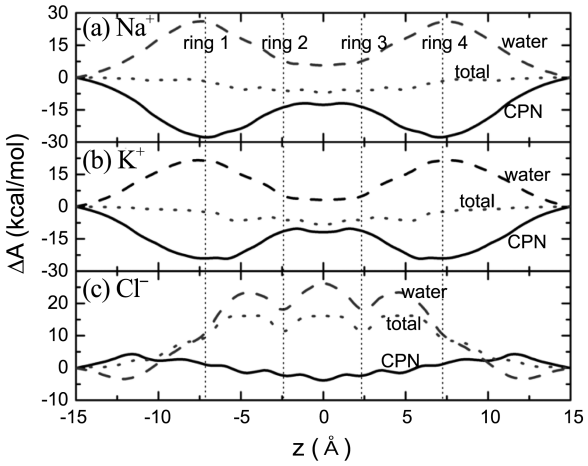

Figure 4. Mean force decomposition profiles representing the contribution of the cyclic peptide nanotube (CPN) and water molecules to the total PMF profiles of (a) Na^+, (b) K^+, and (c) Cl^-. The mean force decomposition profiles were obtained using the TI method.

each window. In many PMF calculation studies based on the US method, sampling periods of 0.5 to 1.0 ns in each window are popularly used.[5,31-33] Our study shows that much caution about the sampling period should be taken for PMF calculations of ions permeating through natural ion channels that are even more complex than cyclic peptide nanotubes.

Figure 3 shows the PMF profiles for a single Na^+, K^+, or Cl^- ion as a function of the ion position in the *z* direction parallel to the channel axis. The PMF profiles obtained from the US method have an excellent agreement with the profiles obtained using the TI methods. The PMF curves of the Na^+ and K^+ exhibit free energy wells in the middle of the channel, while the PMF profile of the Cl^- features a free energy barrier. Comparison of the three PMF profiles indicates that the cyclic peptide nanotube is selective to cations rather than anions, which was confirmed by experimental results by Sánchez-Quesada *et al.*[34] The comparison also reveals that the cations are more stabilized in the midplane regions than in the alpha-plane regions, whereas the Cl^- has the lower free energy barrier in the alpha-plane regions than the midplane regions. A free energy barrier of 16.3 kcal/mol in the PMF profile of the Cl^- is high enough to prevent any single anion from permeating through the channel. The PMF profiles for the cations display local minima in the the midplane regions, implying that the cations can remain for a while during translocation through the peptide nanotube. On the contrary, the PMF curve for the Cl^- shows local minima in the alpha-plane regions. The PMF curve of K^+ has a deeper energy well as compared to the PMF profile of Na^+, which requires a further study on the relation between the PMF profiles and ion conductance.

The mean force decomposition profiles in Figure 4 represent the contribution to the total PMF profiles from each component in the system, i.e., the peptide nanotube and water molecules. In the case of Na^+ and K^+, the relatively flat total PMF profiles arise from the cancellation of very large opposing contributions from the tube and water molecules. The PMF decomposition profiles for the cations demonstrate that as the cations approach the channel entrance, an attractive contribution from the peptide tube increases, whereas the favorable contribution from the water decreases. The lowering of the total PMF profiles by the contribution from the peptide nanotube can be ascribed to negatively charged dangling carbonyl oxygens attached to the outermost rings because an attractive interaction between a cation and the relatively freely moving carbonyl oxygens can stabilize the cation. As a cation comes close to the channel entrance, several water molecules hydrating the cation must be taken apart. The so-called desolvation process gives rise to the unfavorable contribution to the total PMF by the water molecules, leading to the increase in the mean force decomposition profile corresponding to water. The attractive contribution by the peptide nanotube decreases inside the channel as compared to the free energy at the channel entrance. Outside the channel entrance, an attractive interaction of a cation with the dangling carbonyl oxygens in the outermost ring units stabilize the cation. In side the channel, however, the carbonyl oxygens in the rings participate in the hydrogen bonding with other rings as well as the interaction with the cation. As a result, the stabilization of the cation by the carbonyl oxygens is somewhat reduced, leading to the decrease of the attractive contribution by the nanotube inside the channel. The contribution to the total PMF profiles by water molecules inside the channel increases because water molecules have more favorable interactions with the cations in the absence of the dangling carbonyl oxygens. However, the overall contribution by water molecules inside the nanotube are still unfavorable, which introduces free energy barriers of 3-5 kcal/mol in the middle of the nanotube. Consequently, the stabilization of the cations inside the peptide nanotube, indicated by the negative total free energy differences, appears to be esta-

blished by the cyclic peptide nanotube rather than water molecules.

Figure 4(c) shows that the PMF for the Cl^- is dominated by a unfavorable contribution from water molecules rather than the nanotube. As a Cl^- ion approaches the channel entrance, the contribution from the peptide nanotube becomes unfavorable whereas the contribution from the water molecules is attractive. The unfavorable contribution from the peptide nanotube can be attributed to the repulsive interaction between the anion and the dangling carbonyl oxygens. Although there are also positively charged dangling hydrogen atoms in the outermost rings, the interaction between Cl^- and the hydrogen atoms is overwhelmed by the more negative carbonyl oxygens. Inside the channel, the unfavorable interaction of the anion with the carbonyl oxygens is turned into a favorable contribution of −3.8 kcal/mol from the nanotube in the middle of the channel due to the participation of the carbonyl oxygens in the hydrogen bonding. Water molecules inside the channel produce free energy barriers which rapidly increases up to 26 kcal/mol in the middle of the channel. The free energy barriers induced by water is the origin of the energy barrier in the total PMF for Cl^-. Overall, the desolvation of water molecules inside the cyclic peptide nanotube leads to free energy barriers of 3-5 kcal/mol for Na^+ and K^+, and of 26 kcal/mol for Cl^-. In the case of the cations, the free energy barriers are completely compensated for by an attractive interaction between the cations and the carbonyl oxygens in the peptide nanotube. For Cl^-, the favorable contribution from the nanotube to the free energy is minimal and can not eliminate the free energy barriers by water molecules, resulting in the high free energy barriers in the total PMF profile.

The contributions from the cyclic peptide nanotube and water molecules to the total PMF profiles can be examined by calculating the coordination number of an ion with oxygen atoms pertaining to either water molecules or carbonyl groups in the peptide nanotube within the first solvation shell around the ion. The radii of the first solvation shell of water molecules around an ion were obtained by performing separate MD simulations for the three ions in bulk water and by calculating the radial distribution functions. The first solvation shell radii for Na^+, K^+, and Cl^- are determined to be 3.1 Å, 3.6 Å, 3.9 Å, respectively. Figure 5 represents the coordination number of each ion with oxygen atoms either in water molecules or in carbonyl groups inside the peptide nanotube. In the case of cations, the number of chelating carbonyl oxygen atoms increases up to three or four atoms in the mid-plane regions while the number of water oxygen atoms increases in the alpha-plane regions. The increase of the number of the carbonyl oxygen atoms in the midplane regions corresponds to the minima in the total PMF profiles, confirming the stabilization of the cations by the peptide nanotube. It is found out in Figure 5(a) and (b) that the dehydration of water molecules from the cations inside the nanotube is made up for by the replacement of the carbonyl oxygen atoms in the cyclic peptide nanotube. As shown in Figure 5(c), the number of the carbonyl oxygen atoms found in the first solvation shell around a Cl^- ion is minimal due to the repulsive electrostatic interaction between the anion and the carbonyl oxygen atoms.

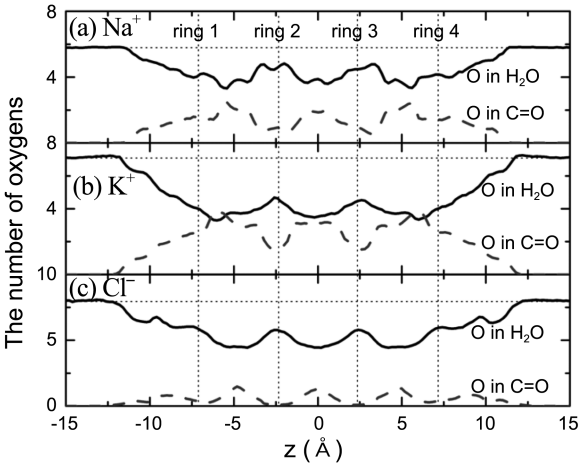

Figure 5. Number of oxygen atoms belonging to either water molecules or carbonyl groups inside the first solvation shell around each ion. The horizontal broken lines indicate the coordination number of water oxygen atoms inside the first solvation shell around the ions in a bulk water.

Concluding Remarks

In this work we demonstrated the ion selectivity of a synthetic ion channel on the basis of the free energy variation. We utilized both the US and TI methods to obtain and compare the PMF profiles of Na^+, K^+, and Cl^- through a simple cyclic peptide nanotube. The final PMF profiles independently acquired from the two methods show an excellent agreement with each other. Comparison of the final PMF profiles with the individual PMF profiles suggests that the PMF calculations should be performed with caution for ion transport through natural ion channels that are much more complex than the system in this study. The PMF profiles for Na^+ and K^+ ions feature free energy wells while the PMF profile for a Cl^- ion shows free energy barriers, indicating the selectivity of the cyclic peptide nanotube to cations. The mean force decomposition profiles for Na^+ and K^+ ions indicate the desolvation mechanism of water molecules near the channel entrance and inside the channel which is completely compensated for by an attractive interaction between the cations and the carbonyl oxygens in the nanotube. In the case of Cl^-, however, the desolvation free energy barriers by water molecules are not eliminated by a relatively negligible interaction between the anion and the peptide nanotube, leading to the high free energy barriers in the total PMF profile of Cl^-. Calculation of the coordination number of the ions with oxygen atoms pertaining to either water molecules or carbonyl groups in the peptide nanotube reveals that the stabilization of the cations in the midplane regions of the nanotube arises from the interaction of the cations with the negatively charged carbonyl oxygens. Although the PMF calculations in this work have been done using a simple synthetic ion channel, we believe that the

results from this work will provide useful insight for understanding the ion selectivity in natural ion channels.

Acknowledgments. This research was supported by Basic Science Research Program through the National Research Foundation of Korea (NRF) funded by the Ministry of Education, Science and Technology (No. 2009-0065893 and No. 2009-0087013). This research was supported by the Kangwon National University (No. 120070284).

References

1. Voet, D.; Voet, J. G. *Biochemistry*, 3rd ed.; John Wiley & Sons, Inc.: 2004; Vol. 1.
2. MacKinnon, R. *Angew. Chem. Int. Ed.* **2004**, *43*, 4265.
3. Hille, B. *Ionic Channels of Excitable Membranes*, 3rd ed.; Sinauer Associates, Inc.: Sunderland, Massachusettes, 2001.
4. Roux, B. *J. Phys. Chem.* **1991**, *95*, 4856.
5. Allen, T. W.; Andersen, O. S.; Roux, B. *Proc. Natl. Acad. Sci. USA* **2004**, *101*, 117.
6. Zhang, D.; Gullingsrud, J.; McCammon, J. A. *J. Am. Chem. Soc.* **2006**, *128*, 3019.
7. Lee, J.; Im, W. *Phys. Rev. Lett.* **2008**, *100*, 018103.
8. Ghadiri, M. R.; Granja, J. R.; Milligan, R. A.; McRee, D. E.; Khazanovich, N. *Nature* **1993**, *366*, 324.
9. Ghadiri, M. R.; Granja, J. R.; Buehler, L. K. *Nature* **1994**, *369*, 301.
10. Ghadiri, M. R.; Kobayashi, K.; Granja, J. R.; Chadha, R. K.; McRee, D. E. *Angew. Chem. Int. Ed. Engl.* **1995**, *34*, 93.
11. Motesharei, K.; Ghadiri, M. R. *J. Am. Chem. Soc.* **1997**, *119*, 11306.
12. Kim, H. S.; Hartgerink, J. D.; Ghadiri, M. R. *J. Am. Chem. Soc.* **1998**, *120*, 4417.
13. Fernadez-Lopez, S.; Kim, H. S.; Choi, E. C.; Delgado, M.; Granja, J. R.; Khasanov, A.; Kraehenbuehl, K.; Long, G.; Weinberger, D. A.; Wilcoxen, K. M.; Ghadiri, M. R. *Nature* **2001**, *412*, 452.
14. Sánchez-Quesada, J.; Ghadiri, M. R.; Bayley, H.; Braha, O. *J. Am. Chem. Soc.* **2000**, *122*, 11757.
15. Engels, M.; Bashford, D.; Ghadiri, M. R. *J. Am. Chem. Soc.* **1995**, *117*, 9151.
16. Asthagiri, D.; Bashford, D. *Biophys. J.* **2002**, *82*, 1176.
17. Tarek, M.; Maigret, B.; Chipot, C. *Biophys. J.* **2003**, *85*, 2287.
18. Khurana, E.; Nielsen, S. O.; Ensing, B.; Klein, M. L. *J. Phys. Chem.* **2006**, page ASAP.
19. Hwang, H.; Schatz, G. C.; Ratner, M. A. *J. Phys. Chem. B* **2006**, *110*, 26448.
20. Dehez, F.; Tarek, M.; Chipot, C. *J. Phys. Chem. B* **2007**, *111*, 10633.
21. MacKerell, A. D., Jr.; Bashford, D.; Bellott, M.; Dunbrack, R. L., Jr.; Evanseck, J.; Field, M. J.; Fischer, S.; Gao, J.; Guo, H.; Ha, S.; Joseph-McCarthy, D.; Kuchnir, L.; Kuczera, K.; Lau, F. T. K.; Mattos, C.; Michnick, S.; Ngo, T.; Nguyen, D. T.; Prodhom, B.; III, W. E. R.; Roux, B.; Schlenkrich, M.; Smith, J. C.; Stote, R.; Straub, J.; Watanabe, M.; Wiorkiewicz-Kuczera, J.; Yin, D.; Karplus, M. *J. Phys. Chem. B* **1998**, *102*, 3586.
22. Jorgensen, W. L.; Tirado-Rives, J. *J. Am. Chem. Soc.* **1988**, *110*, 1657.
23. Beglov, D.; Roux, B. *J. Chem. Phys.* **1994**, *100*, 9050.
24. Phillips, J. C.; Braun, R.; Wang, W.; Gumbart, J.; Tajkhorshid, E.; Villa, E.; Chipot, C.; Skeel, R. D.; Kale, L.; Schulten, K. *J. Comp. Chem.* **2005**, *26*, 1781.
25. Humphrey, W.; Dalke, A.; Schulten, K. *J. Mol. Graphics* **1996**, *14*, 33.
26. Roux, B. *Comp. Phys. Comm.* **1995**, *91*, 275.
27. In *Free Energy Calculations*; Chipot, C., Pohorille, A., Eds.; Springer: Berlin, 2007.
28. Tuckerman, M. E. *Statistical Mechanics: Theory and Molecular Simulation*; Oxford University Press: Oxford, 2010.
29. Roux, B.; Karplus, M. *Biophys. J.* **1991**, *59*, 961.
30. Grossfield, *A. version 2.0.4, http://membrane.urmc.rochester.edu/content/wham* 2010.
31. Leung, K.; Rempe, S. B.; Lorenz, C. D. *Phys. Rev. Lett.* **2006**, *96*, 095504.
32. Chang, R.; Violi, A. *J. Phys. Chem. B* **2006**, *110*, 5073.
33. Song, C.; Corry, B. *J. Phys. Chem. B* **2009**, *113*, 7642.
34. Śanchez-Quesada, J.; Isler, M. P.; Ghadiri, M. R. *J. Am. Chem. Soc.* **2002**, *124*, 10004.